ChemPubSoc Europe

DOI: 10.1002/open.201900183

Open Access ChemistryOPEN Full Papers

Robust Aluminum Electrodeposition from Ionic Liquid Electrolytes Containing Light Aromatic Naphta as Additive

Elena Guinea,*[a] Asier Salicio-Paz,[a] Aitor Iriarte,[a] Hans-Jürgen Grande,[a] Estíbaliz Medina,[b] and Eva García-Lecina[a]

Aluminum electrodeposition can be carried out from several ionic liquid electrolyte formulations. Nevertheless, this plating process has not been industrialized so far because of the durability of the electrolytes and because the Al coatings obtained are non-fully homogeneous in terms of coating morphology and thickness distribution. In this work we electrodeposited Al coatings from a 3-butyl-1-ethylimidazolium tetrachloroaluminate electrolyte additivated with increasing concentrations of a new cost-effective additive: light aromatic naphtha solvent. Firstly, electrolytes were characterized by cyclic voltammetry, where changes in the electrochemistry of the process were identified. Then, surface characterization showed that Al coatings morphology turned out to be smoother, more homogeneous and more compact with increasing additive concentration. Furthermore, the process was scaled up to flat plates of 18 cm^2 area and also on 25 cm^2 parts designed with straight corners to demonstrate both the optimization of the electrolytic bath performance and its throwing power enhancement.

1. Introduction

Metal electroplating from ionic liquids, eutectic formulations and molten salts has been extensively studied in the last years.[1–6] These non-aqueous solutions have gained interest because of their non-volatility and inflammability, good solubility, high stability and their wide electrochemical window.[7] This last feature has paved the way to investigate novel metal coatings which are not possible to obtain from aqueous solutions,[8] mainly because their reduction potential is more negative than the reduction potential of water to hydrogen. Among these electronegative metals, aluminum, magnesium or titanium have aroused keen interest for industrial applications because of their valuable properties. As far as aluminum concerns, its lightweight, thermal conductivity and its corrosion protection properties attract the attention of many industrial sectors.[9,10]

In the last years, aluminum has been successfully electrodeposited from several ionic liquid electrolytes, most of them formed by the eutectic combination of $AlCl_3$ and imidazolium or pyrimidinium chloride salts.[11–18] However, in spite of having demonstrated the viability of electrodepositing coatings of highly pure aluminum on different metallic surfaces,[11,15,19–23] the process is still not optimized. Thus, the obtained coatings are matt and non-homogeneous and regularly exhibit dendritic crystals or burned areas on the cathode surface. Moreover, these drawbacks are emphasized in case of large or complex 3D-shaped parts, usually produced in real industrial applications, because of the poor throwing power of these electrolytes. Furthermore, when increasing current density or coating thickness, the coatings easily peel off .[24]

Different strategies have been investigated in order to obtain homogeneous Al deposits with proper microstructure. Thus, Reddy et al.[19] demonstrated the influence of electrode surface and cathode overpotential in the growth of Al coatings. They reported that Al electrodeposition on copper substrates took place in two steps. First, a thin layer of Al is deposited onto copper. This electrodeposited Al forms an alloy with Cu by inter-diffusion. Once the intermetallic layer is saturated, dendritic Al grows up. Regarding electrochemical process parameters, on one hand it is known that electrodeposition in these electrolytes is facilitated at high temperatures as they enhance ions movement. On the other hand, it turned out that low content of aluminum chloride in the melt and high voltages gave a uniform particle size distribution in the aluminum deposits.[25] This favourable surface morphology is attributed to changes in the Lewis acidity of the melt resulting from the depletion of $Al_2Cl_7^-$ species at the electrode surface during the reduction reaction. Concerning the electrolyte composition, species evolution/degradation caused by the cation reduction reactions seems to be another key factor.[26] In this regard, Endres et al.[17] reported that nano-crystalline aluminum in chloroaluminate eutectics is only formed if there is enough decomposition of the cation (3-ethyl-1-methylimidazolium in their study), which is also responsible for the colour changes observed in these electrolytes after current passing for few

[a] E. Guinea, A. Salicio-Paz, A. Iriarte, H.-J. Grande, E. García-Lecina
CIDETEC,
Parque Científico y Tecnológico de Gipuzkoa
P° Miramón, 196
20014 Donostia-San Sebastián, Spain
E-mail: eguinea@cidetec.es
[b] E. Medina
MTC – Maier Technology Centre
Polígono Industrial Arabieta
B° Kanpantxu S/N
48320 Ajangiz-Bizkaia, Spain

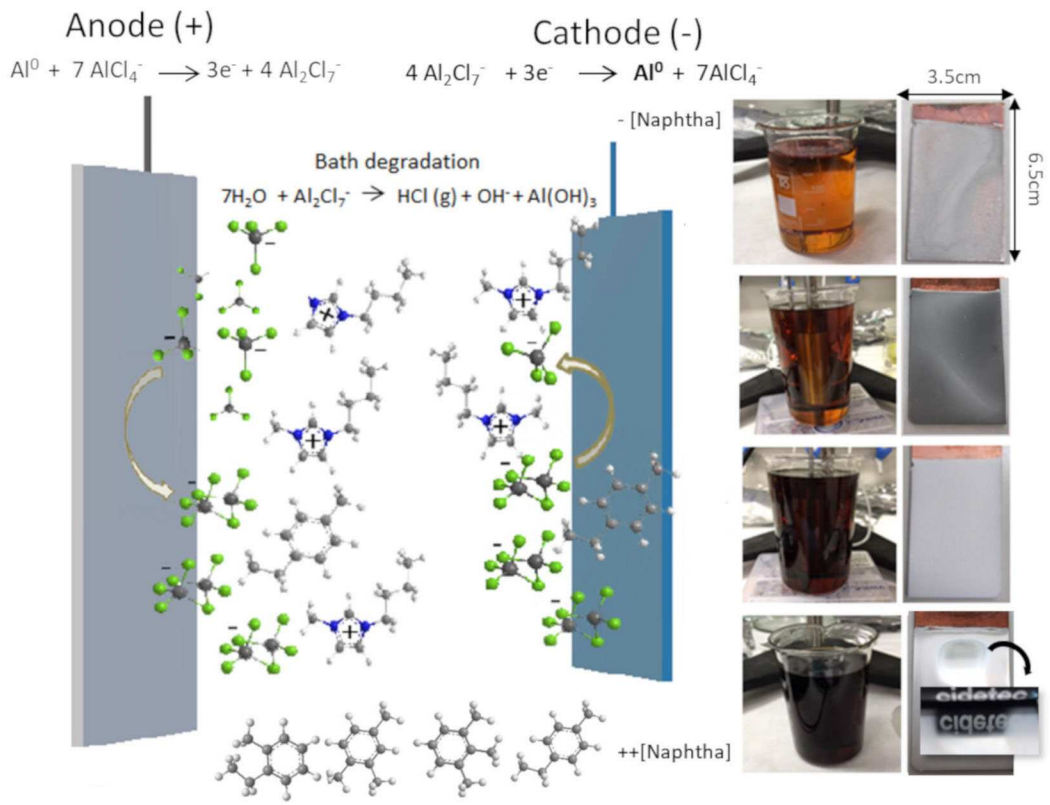

Figure 1. Left) Scheme of Al electroplating process. Right) Colour shift of the [BMIm]Cl/$AlCl_3$ electrolyte at different additive concentrations and respectively Al plated parts.

minutes. This investigation opened the door to further research about the use of additives/brighteners in electrodeposition from ionic liquids. Thus, the influence of some additives including alkali metals and rare earths chlorides, surfactants and also organic solvents (N-hexane, cyclohexane, toluene and ammonia chloride) on the Al deposition from eutectic [BMIm]Cl/$AlCl_3$ has been recently studied by Zhang, S. et al.[16] According to the authors, inorganic additives could alter the speciation of aluminum meanwhile small organic molecules are promising additives to obtain uniform and dense aluminum coatings. They also pointed out that organic additives cannot be co-deposited with Al, which is one of the main advantages as it guarantees the purity of the Al coating. The mechanism whereby toluene influences the electrodeposition is related with benzene ring structure and the presence of double bonds. Xylene[23,25] toluene[27] (30% v/v) and benzene (50% v/v)[28,29] have been also considered as co-solvents for obtaining homogeneous and mirror-bright Al deposits. The presence of the co-solvent promotes lower viscosity and higher conductivity in the electrolyte, in comparison with bare melts, facilitating the plating process. Regarding the use of organic additives as brighteners, nicotinic acid and methyl nicotinate (2.0 to 8.0 mmol)[30,31] have given good results on small flat surfaces (10 mm × 10 mm) whereas 1,10-phenantroline (27.7 mmol)[32] was tested on car wheel bolts.

In this work we report for the first time the effect of adding to the eutectic [BMIm]Cl/$AlCl_3$ a cost effective organic light aromatic naphtha solvent as additive (from 2.4 to 9.7 mmol). Results demonstrate the enhancement of the electrolyte performance (homogeneity and grain size of the aluminum coatings and throwing power of the electrolyte) in the presence of low concentrations of naphtha compared to previously reported organic solvents (0.03–0.15% v/v vs 25–50% v/v for toluene or benzene). Moreover, this optimised electrolyte leads to very homogenous, adherent and compact Al coatings allowing tailoring grain morphology depending on the concentration of the naphtha additive. Additionally it enhances the throwing power allowing the electrodeposition on 3D-shaped components.

2. Results and Discussion

2.1. Composition of the Electrochemical Bath

The electrolyte used in this work is the eutectic 3-butyl-1-ethylimidazolium tetrachloroaluminate melt additivated with light aromatic naphtha solvent, which is a mixture of ethyl-toluene and trimethylbenzene (see Figure 1).

There is no other solvent so that the ions are subjected to electrostatic forces in a randomness environment. When current is applied to the electrolyte (Figure 1), cations ($BMIm^+$) tend to move towards the cathode (−) while anions (Al (III) complexes) tend to move to the anode (+). As the electroactive specie

($Al_2Cl_7^-$) is negatively charged, forced convection is crucial to help it reaching the cathode's surface. Once there, $Al_2Cl_7^-$ is reduced to Al (0) and $AlCl_4^-$ while Al (0) is oxidized at the anode to Al (III), giving rise to different complexes with Cl^-. Thus, the electroactive species are regenerated by Al dissolution and reaction with $AlCl_4^-$.[20]

As it is shown on the right side of Figure 1, the non-additivated electrolyte (blank) is light-brown/orange coloured. The coatings obtained from this formulation are matt and dendritic, and copper from the substrate can be easily spotted at some areas of the surface by the naked eye. When light aromatic naphtha is added to the electrolyte (1.2 mmol) the electrolytic bath turns darker. In this case, Al coating covers the entire copper surface but a lack of homogeneity is still detectable. For the dark brown 2.4 mmol (not shown) and the very dark brown 3.6 mmol electrolytes, deposits obtained are smoother and highly homogeneous. Finally, for the 9.7 mmol electrolyte (very black coloured) the grain size decreased and bright-mirror areas are observed on the surface.

Why light aromatic naphtha additive helps in this process is still not clear. No changes in the viscosity neither in the conductivity of the electrolytes with the studied additive concentrations were observed. Then, it is postulated that naphtha aromatic molecules form a complex with the Al (III) species present in the electrolyte. This complex formation is probably the responsible for the colour shift in the electrolyte from orange to very dark brown colour when it is added to the [BMIm]Cl/$AlCl_3$ (1.0/1.5 M). Thus, these colour changes are related to changes in the coordination environment of the Al(III) species. Consequently, for the $Al_2Cl_7^-$ anions coordinated to aromatics, it could be possible to delocalize the negative charge so that it would enable its electrode approximation. Nevertheless, the complex dimension could also be a drawback to reach the electrode surface, ordering the nucleation and the growth of the Al deposit. Abbott et al.[27] also observed that the colour of some ionic liquid based electrolytes becomes darker with the addition of toluene and they attributed it to neutral charge-transfer complex $AlCl_3$ (toluene). Moreover, as these authors mentioned, formation of this complex could be related with the increase in concentration of $Al_2Cl_7^-$. On the contrary, these colour changes are not observed for other studied additives such as nicotinamide.[24] In that case, the authors indicated that nicotinamide has no influence on the coordination environment of Al (III) and the mechanism proposed was that nicotinamide is absorbed onto the electrode surface inhibiting the electrochemical reaction. Therefore, the reduction potential was observed to move into more negative values. The same was observed for the 1,10-phenantroline additive,[33] where authors reported a slow down on the deposition rate and also changes in the nucleation and growth mechanism in presence of this additive. At that point, to investigate how the presence of light aromatic solvent naphtha affects the electroreduction mechanism of our system, we characterized the electrolyte by cyclic voltammetry.

2.2. Cyclic Voltammetry

Cyclic voltammetry was used as a first diagnosis analysis in order to verify the electronic transfer at the electrode and the current density of the process for each electrolyte tested. Figure 2 shows the voltammograms recorded on a 3 mm disc Pt

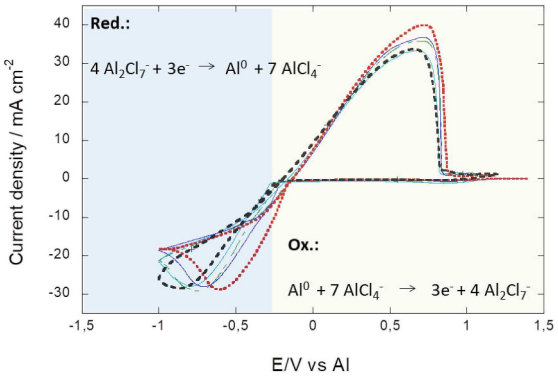

Figure 2. Cyclic Voltammogram of Al deposition on Pt substrate (3 mm diameter) at T = 50 °C, scan rate 50 mV s^{-1} in eutectic BMIMCl/$AlCl_3$ (1/1.5 M) without additives (dashed black) and with increasing concentration of naphtha aromatic solvent: 1.2 mmol (green), 2.4 mmol (light blue), 3.6 mmol (dark blue) and 9.7 mmol (dashed red).

electrode immersed into the BMIMCl/$AlCl_3$ (1/1.5 mol) electrolyte. The potential scan started at OCP (open circuit potential) to −1.0 V vs. Al, where Al (III) complex is reduced to Al (0). Then, the potential goes to 1.5 V vs. Al at 50 mVs^{-1} scan rate. As it can be seen for the non-additivated electrolyte (black dashed), the Al electrodeposition (reduction) starts at −0.24 V vs. Al, and reaches the E_{pc} (cathodic peak potential) at −0.87 V vs. Al. At this potential, the concentration of electroactive species near the electrode decreases and therefore current density decays. At the anodic sweep we can observe another electronic transference which corresponds to the oxidation of the Al (0) electrodeposited during the cathodic sweep (anodic peak potential (E_{pa}) = 0.68 V vs. Al). As we can observe in Figure 2, in the presence of light aromatic naphtha additive, the cathodic potential turns out to be less negative. For electrolytes 1.2 mmol, 2.4 mmol and 3.6 mmol E_{pc} decreases to around −0.75 V vs. Al. Then, for the most concentrated electrolyte (9.7 mmol), the Al electrodeposition starts at −0.16 V vs. Al reaching the E_{pc} at −0.61 V vs. Al. Thus, in the studied range of concentrations, the higher the concentration of naphtha aromatic solvent, the less negative is E_{pc}. This would mean that the reduction process is being facilitated.

2.3. Aluminum Coatings Characterization

The above-mentioned solutions were used as electrolyte for Al electrodeposition on ABS-Cu coated substrates of 18 cm^2 area (Figure 1). It is noticeable that the deposit obtained in presence of the additive is much homogeneous and smoother. The reduced surface roughness was also evidenced by surface and

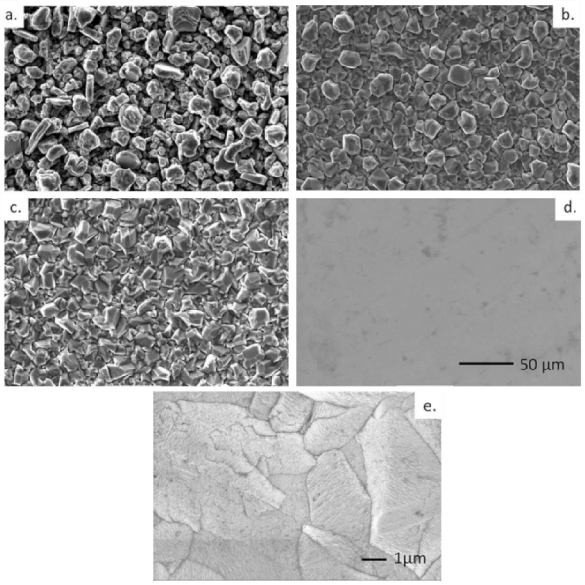

Figure 3. SEM images of the Al coatings deposited from electrolyte BMIMCl/$AlCl_3$ (1/1.5 M) increasing light aromatic naphtha concentrations: a.1.2 mmol, b. 2.4 mmol, c. 3.6 mmol, d. 9.7 mmol, and FE-SEM image: e. 9.7 mmol.

Figure 4. Cross section FESEM images of Al coatings deposited from the BMIMCl/$AlCl_3$ (1/1.5 M) a. non-additivated and b. 9.7 mmol light aromatic naphtha additivated.

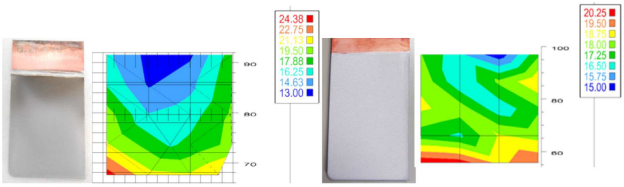

Figure 5. XRF thickness mapping for Al coatings obtained from non-additivated (left) and 3.6 mmol light aromatic naphtha additivated (right) electrolytes.

cross section characterization. As it is shown in SEM and FESEM images (Figure 3) the grain size of the Al deposits decreases as the light aromatic naphtha concentration in the electrolyte increased. From the 1.2 mmol to the 2.4 mmol and 3.6 mmol additive concentration, the grain size is gradually smaller and more compact, whereas at 9.7 mmol there are no grains visible at the same magnification using the SEM. The FE-SEM analysis of the coating obtained at 9.7 mmol naphtha concentration (Figure 3-e) revealed the very compact small grains of the aluminum coating (bright area).

Cross section characterization shows clear differences between the coatings obtained from the studied electrolytes. With non-additivated electrolytes, Al coatings are rough and irregular (Figure 4a.). The surface becomes more uniform increasing additive concentration in the electrolyte up to 9.7 mmol (see Figure 4b.) where we can observe that there is an evident decrease of the roughness, higher compactness and better adhesion to the substrate. The thickness of the coatings was measured both by FE-SEM cross section evaluation and by non-destructive X-Ray fluorescence. Al coatings average thickness was around 20 µm in all the cases (Figure 5).

Figure 6 shows the XRD patterns of Al coatings obtained from BMIMCl/$AlCl_3$ (1/1.5 M) in the presence of increasing

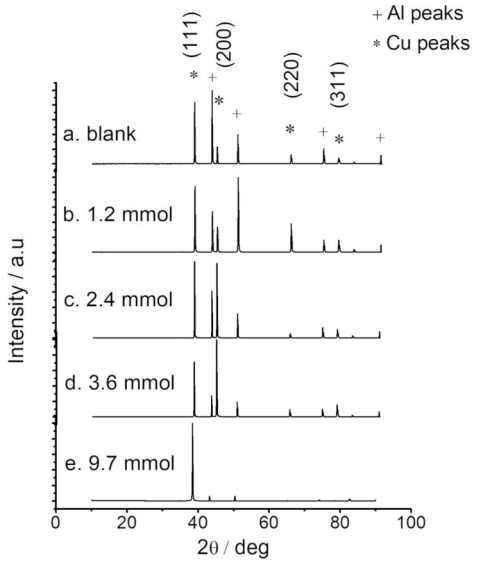

Figure 6. XRD patterns of Al coatings deposited from a) BMIMCl/$AlCl_3$ (1/1.5 M) and b-e) increasing light aromatic naphtha concentrations. Diffraction peaks are denoted with circles for Al and squares for Cu substrate.

concentrations of light aromatic naphtha additive up to 9.7 mmol. Four Al crystallographic peaks were identified according to JCPDS card Al (00-004-0787), while the rest of the peaks were attributed to the copper substrate. Furthermore, texture coefficients, TC (hkl) of the 4 crystallographic planes (111), (200), (220) and (311) were calculated according to equation (1):

$$TC(hlk) = \frac{\frac{Ihlk}{Irhlk}}{\frac{1}{n}\sum\left(\frac{Ihlk}{Irhlk}\right)} \quad (1)$$

Where I_{hlk} is the peak intensity of the obtained deposits, I_{rhlk} is the peak intensity of the crystallographic plane for the JCPDS card n° 00-004-0787 and n is the number of total crystallographic planes considered.

The calculated TCs are listed in Table 1:

Additionally, the average grain size of Al was determined from the full width at half maximum (FWHM) of the most intense peak according to the Scherrer equation (2).

$$D = (K.\lambda\ )/(\beta\ cos\theta) \quad (2)$$

According to these data (Table 1), aluminum crystal size seems not to be strongly affected by the presence of this additive in the different concentrations tested, being in the range 65–77 nm.

On the other hand, it can be seen both in Table 1 and Figure 6, that light aromatic naphtha concentration influences the nano-crystallinity of the Al deposits. The distribution of crystallographic orientations of the polycrystalline aluminum deposits change from fully random oriented crystals to a more textured growth as most of the Al crystals exhibit a (111) preferred orientation for the BMIMCl/$AlCl_3$ (1/1.5 M) 9.7 mM light aromatic naphtha additivated electrolyte. In this case, the relative intensity of the (111) reflection increases dramatically, whereas the intensities of the (311), (200), and (220) reflections decrease. As it is shown in (Figure 6e) on brighter areas, all peaks are vanished except for the (111) preferred orientation. Moreover, according to what we have previously observed on SEM and FE-SEM images, Al coatings are so compact that copper peaks (substrate) are attenuated. On the contrary (200) crystallographic preferred orientation is observed for the intermediate 2.4 mmol and 3.6 mmol additivated electrolytes. This variations on crystallographic orientations as function of additives, temperature or even applied current density has been already reported by several authors.[24,31,34,35]

2.4. Throwing Power of the Electrolytes

Lastly, we compared the throwing power of the non-additivated and light aromatic naphtha additivated electrolyte, as it is a mayor issue for process industrialization purposes. Thereby, throwing power is a measure of the ability of an electroplating solution to plate onto a uniform thickness over an irregularly shaped cathode. To this end, copper plates were shaped as it is shown in Figure 7. As it is shown in Figure 7, the electrolyte additivated with light aromatic naphtha has better throwing power as more surface area is plated, including hindered or recessed areas.

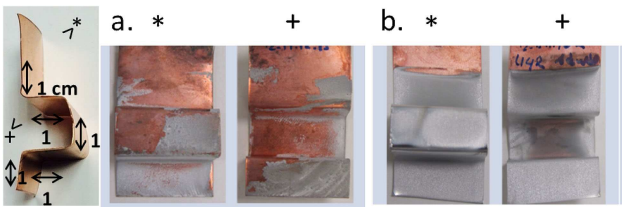

Figure 7. Throwing power experiments: Al coatings deposited from electrolyte BMIMCl/$AlCl_3$ (1.0/1.5 M) a) without additives b) 3.6 mmol light aromatic naphtha.

3. Conclusions

In this work, we have presented the effect of a new additive for 1-butyl-3-methylimidazolium tetrachloroaluminate BMIMCl/$AlCl_3$ (1/1.5 M) plating baths. The light aromatic naphtha additive added to the mentioned ionic liquid (1.2, 2.4, 3.6 and 9.7 mmol) was tested for the electrodeposition of aluminum onto large size and 3D-shaped copper parts at 50 °C. In presence of this additive, the reduction process is being facilitated as the cathodic peak shifts towards the less negative values, while there is an enhancement in the morphology and homogeneity of the electrodeposited Al coatings. Moreover, it has been demonstrated that the grain size of the Al deposits can be modified varying the light aromatic naphtha additive concentration. Thus, it is possible to tailor the surface microstructure of the coatings just adding different concentrations of the additive studied. Besides, the distribution of crystallographic orientations of the aluminum deposits change from fully random to moderately textured, exhibiting a (111) preferred orientation, particularly for bright Al deposits. Furthermore, the plating process was scaled up to 25 cm^2 area curved parts designed with straight corners, were the additive-driven enhancement of the throwing power of the modified electrolyte has been demonstrated.

Experimental Section

The electrolyte for aluminum electrodeposition was synthesized by carefully mixing [BMIM]Cl (1-Butyl-3-methylimidazolium chloride) 99.0% supplied by IOLITEC and aluminum chloride supplied by ACROS ORGANICS (molar ratio 1:1.5) at room temperature in a dry room (dew point average −56 °C). Additives were introduced to the electrolyte once it was perfectly mixed and reached room temperature. Light aromatic naphtha solvent was provided by Molekula.

All electrochemical studies with the ionic liquid electrolyte were carried out in a dry room using an Autolab model PGSTAT30 potentiostat/galvanostat fitted with a conventional three-electrode glass cell (50 mL baker, solution volume 20 mL for voltammetry and 150 mL beaker, solution volume 150 mL for electrodeposition essays). Voltammetry essays were conducted in a three-electrode system in non-stirred solutions at a temperature of 25 and 50 °C. Pt disc (1.5 mm radius) was used as working electrode, Pt (99.99%, Good fellow) and Al wire (99.99%, ALFA AESAR) as reference electrodes and Al foil (99.99% Alfa Aesar and 99.5% Al AA1050 alloy, which contains Fe (<0.40%) and Si (<0.25%) as main alloying elements) as counter electrodes. The Pt working electrode was polished with 0.3 mm alumina paste, washed by deionized

Table 1. Texture coefficients and average crystal size of the Al deposits obtained by electrodeposition from BMIMCl/$AlCl_3$ 1.0/1.5 mol electrolyte additivated with light aromatic naphtha.

Electrolyte	TC (111)	TC (200)	TC (220)	TC (311)	D (nm)
Blank (BMIMCl/$AlCl_3$ 1.0/1.5 M)	1.93	1.1	0.13	0.84	64.99
1.2 mmol	0.85	0.72	1.77	0.66	65.38
2.4 mmol	1.14	2.38	0.31	0.17	76.70
3.6 mmol	0.72	2.17	0.45	0.66	77.32
9.7 mmol	4.0	0.00	0.00	0.00	75.27

water, and dried prior to all measurements. Electroplating experiments were carried out in a two-electrode system in well stirred solutions under argon bubbling at 50 °C temperature, $j = 1.5$ Acm^{-2} for 2 hours. Additive concentration should be refilled after 4 to 10 hours operating of the electrolytic bath due to its evaporation or its incorporation to the coating. ABS coppered plate (1–9 cm^2 area) was used as working electrode and Al foil (99.99% Alfa Aesar and Al AA1050) as counter electrode (1:1 CO:WE area). ABS coppered electrodes plates were activated in an alkaline degreasing (UNI-CLEAN), then in HNO_3 15% and carefully dried with paper and air before introducing into the electrolyte. Al electrodes were activated in NaOH (50% w/v), then washed in ultrapure water and finally dried thoroughly with pressurized air.

The throwing power experiments were carried out using 3D-parts of copper as cathode in a two-anode system in well stirred solutions under argon bubbling at 50 °C temperature and at $j =$ 1.0 A·cm^{-2} to avoid burned areas, for 2 hours.

Coatings Characterization

Characterization of Aluminum deposits' surface-cross section morphology and chemical composition was carried out on a JEOL JSM-5500LV Scanning Electron Microscope – energy dispersive X-ray spectrometry (SEM-EDS) and a ZEIS ULTRA plus Field emission scanning electron microscope (FESEM). An X-ray diffraction (Bruker D8 Advance) was used for crystallographic characterization of the coatings. A FISCHERSCOPE X-RAY XDV-SDD (XDAL-FD) measuring instrument was used as non-destructive characterization of both composition and thickness of the coatings as it provides a very useful map of thickness distribution for the aluminum layer.

Acknowledgements

The authors would like to express their gratitude to the Basque Government for supporting this collaborative research by the ELKARTEK grant, projects: Al_LI+D (KK-2017/00034) and FRONTIERS IV (KK-2018/00108) and would like to thank Professor David Mecerreyes for fruitful discussions.

Conflict of Interest

The authors declare no conflict of interest.

Keywords: metal electroplating · Al coating · electrodeposition · ionic liquids · naphtha · scanning electron microscopy

[1] Q. Zhang, Q. Wang, S. Zhang, X. Lu, X. Zhang, *ChemPhysChem* **2016**, *17*, 335–351.
[2] A. P. Abbott, G. Frisch, K. S. Ryder, *Annu. Rev. Mater. Res.* **2013**, *43*, 335–358.
[3] M. Galiński, A. Lewandowski, I. Stepniak, *Electrochim. Acta* **2006**, *51*, 5567–5580.
[4] E. L. Smith, C. Fullarton, R. C. Harris, S. Saleem, A. P. Abbott, K. S. Ryder, *Trans. Inst. Met. Finish.* **2010**, *88*, 285–293.
[5] F. Endres, D. MacFarlane, A. Abbott, *Electrodeposition from Ionic Liquids*. Wiley-VCH, Weinheim, **2008**. pp. 83-113..
[6] P. L. Peter, *J. Am. Chem. Soc.* **2008**, *130*, 12549.
[7] W. Simka, D. Puszczyk, G. Nawrat, *Electrochim. Acta* **2009**, *54*, 5307–5319.
[8] F. Endres, *ChemPhysChem* **2002**, *3*, 144–154.
[9] M. Armand, F. Endres, D. R. MacFarlane, H. Ohno, B. Scrosati, *Nat. Mater.* **2009**, *8*, 621–629.
[10] E. M. Moustafa, S. Z. El Abedin, A. Shkurankov, E. Zschippang, A. Y. Saad, A. Bund, F. Endres, *J. Phys. Chem. B* **2007**, *111*, 4693–4704.
[11] T. Jiang, M. J. Chollier Brym, G. Dubé, A. Lasia, G. M. Brisard, *Surf. Coat. Technol.* **2006**, *201*, 1–9.
[12] J. Tang, K. Azumi, *Electrochim. Acta* **2011**, *56*, 1130–1137.
[13] U. Bardi, S. Caporali, M. Craig, A. Giorgetti, I. Perissi, J. R. Nicholls, *Surf. Coat. Technol.* **2009**, *203*, 1373–1378.
[14] L. Gao, L. Wang, T. Qi, Y. Li, J. Chu, J. Qu, *Acta Phys. Chim. Sin.* **2008**, *24*, 939–944.
[15] Y. Zheng, S. Zhang, X. Lü, Q. Wang, Y. Zuo, L. Liu, *Chin. J. Chem. Eng.* **2012**, *20*, 130–139.
[16] L. Liu, X. Lu, Y. Cai, Y. Zheng, S. Zhang, *Aust. J. Chem.* **2012**, *65*, 1523–1528.
[17] F. E. Q. X. Liu, S. Z. El Abedin, *J. Electrochem. Soc.* **2008**, *155*, D357–D362.
[18] T. Jiang, M. J. Chollier Brym, G. Dubé, A. Lasia, G. M. Brisard, *Surf. Coat. Technol.* **2006**, *201*, 10–18.
[19] D. Pradhan, D. Mantha, R. G. Reddy, *Electrochim. Acta* **2009**, *54*, 6661–6667.
[20] E. Berretti, A. Giaccherini, S. M. Martinuzzi, M. Innocenti, T. J. S. Schubert, F. M. Stiemke, S. Caporali, *Materials* **2016**, DOI 10.3390/ma9090719.
[21] P. Giridhar, S. Z. El Abedin, F. Endres, *J. Solid State Electrochem.* **2012**, *16*, 3487–3497.
[22] S. Shiomi, M. Miyake, T. Hirato, A. Sato, *Mater. Trans.* **2011**, *52*, 1216–1221.
[23] Q. X. Liu, S. Z. El Abedin, F. Endres, *Surf. Coat. Technol.* **2006**, *201*, 1352–1356.
[24] Q. Zhang, Q. Wang, S. Zhang, X. Lu, *J. Solid State Electrochem.* **2014**, *18*, 257–267.
[25] T. Tsuda, G. R. Stafford, C. L. Hussey, *J. Electrochem. Soc.* **2017**, *164*, H5007–H5017.
[26] N. DeVos, C. Maton, C. V. Stevens, *ChemElectroChem* **2014**, *1*, 1258–1270.
[27] A. P. Abbott, F. Qiu, H. M. A. Abood, M. R. Ali, K. S. Ryder, *Phys. Chem. Chem. Phys.* **2010**, DOI 10.1039/B917351J.
[28] J.-J. Lee, Y. Mo, D. a. Scherson, B. Miller, K. a. Wheeler, *J. Electrochem. Soc.* **2001**, *148*, C799–C802.
[29] Q. Liao, W. R. Pitner, G. Stewart, C. L. Hussey, G. R. Stafford, *J. Electrochem. Soc.* **1997**, *144*, 936–943.
[30] Q. Wang, Q. Zhang, B. Chen, X. Lu, S. Zhang, *J. Electrochem. Soc.* **2015**, *162*, 320–324.
[31] Q. Wang, B. Chen, Q. Zhang, X. Lu, S. Zhang, *ChemElectroChem* **2015**, *2*, 1794–1798.
[32] L. Barchi, U. Bardi, S. Caporali, M. Fantini, A. Scrivani, A. Scrivani, *Prog. Org. Coat.* **2010**, DOI 10.1016/j.porgcoat.2009.09.025.
[33] L. Barchi, U. Bardi, S. Caporali, M. Fantini, A. Scrivani, A. Scrivani, *Prog. Org. Coat.* **2010**, *68*, 120–125.
[34] S. Z. El Abedin, E. M. Moustafa, R. Hempelmann, H. Natter, F. Endres, *ChemPhysChem* **2006**, *7*, 1535–1543.
[35] F. Endres, M. Bukowski, R. Hempelmann, H. Natter, *Angew. Chem. Int. Ed. Engl.* **2003**, *42*, 3428–30.

Manuscript received: April 27, 2019
Revised manuscript received: July 8, 2019